J. of Supercritical Fluids 50 (2009) 128–137

Contents lists available at ScienceDirect

The Journal of Supercritical Fluids

journal homepage: www.elsevier.com/locate/supflu

Effect of phase behavior in the hydrogenation of triglycerides under supercritical and near-critical propane

C.M. Piqueras*, D.E. Damiani, S.B. Bottini

PLAPIQUI, Universidad Nacional del Sur - CONICET, Camino La Carrindanga km 7; CC 717, 8000 Bahía Blanca, Argentina

ARTICLE INFO

Article history:
Received 27 November 2008
Received in revised form 28 April 2009
Accepted 18 May 2009

Keywords:
Hydrogenation
Propane
Triglyceride
Sunflower oil
Phase behavior

ABSTRACT

Sunflower oil was hydrogenated in a stirred-batch unit, using supercritical and near-critical propane as solvent, and Pd/γ-Al_2O_3 catalyst. The effect of the phase behavior on the reaction performance is analyzed. The transition from homogeneous to heterogeneous conditions showed no effect on the activity and selectivity of the reaction. These results point to an unrestricted availability of hydrogen at the catalyst surface. A comparison is made between fluid–solid mass transfer coefficients in stirred-batch and continuous fixed-bed reactors.

1. Introduction

Supercritical fluids (SCFs) have been applied to catalyzed reactions traditionally carried out in gas–liquid conditions since 30 years ago. Conventionally, these kinds of reactions are carried out under mass-control regime, which limits the catalyst efficiency and the reactor productivity. SCFs overcome these limitations by increasing the solubility of the reaction mixture and improving the mass transfer to the solid catalyst [1]. An important number of heterogeneous catalytic reactions have been performed at lab-scale using SCFs as reaction medium or as reactant and solvent at the same time [1]. The most significant effects observed are improvements in the reaction rate and selectivity, as well as an increase in the catalyst lifetime. These facts, and the easy separation of the SCF from the reaction products, turn this technology attractive for several industrial applications [2].

Quite frequently, supercritical reactions are carried out in blind reactors, with no knowledge on the inside phase conditions. The measured changes in reaction rate and selectivity are often attributed to phase transitions that are not actually verified. Although the importance of phase behavior is generally accepted, its complexities in high-pressure multicomponent systems (i.e. fluid–fluid immiscibility and discontinuities in the critical lines [3]) are often underestimated. Since in many cases the reactants are diluted in the SCF, it is quite common to assume that the phase behavior of the reactive mixture is similar to that of the pure SCF. To disregard the possibility of complex behaviors that may lead to a false interpretation of the observed effects in the rate and selectivity results.

Wandeler et al. [4] stressed the need to know and to control the phase scenario inside the supercritical reactor. Theoretical models proved that were able to get an insight on the reaction process, based on the phase behavior of the reaction mixtures [5].

Due to the increasing concern about the impact of *trans* fatty acids onto human health [6], the exploration of new technologies to minimize their production during hydrogenation is of current interest. In the present work, the catalytic hydrogenation of sunflower oil was carried out in a stirred-batch unit, using propane as reaction solvent. The reactions were performed under homogeneous and two-phase conditions, for hydrogen/oil molar ratios varying between 1 and 10, and covering a temperature range between 323 and 393 K and pressures of 6.5 to 18.3 MPa. The influence of the phase conditions on the reaction rate and selectivity were analyzed.

2. Experimental

2.1. Materials

Propane (99.01% molar; impurities: 0.37% ethane, 0.53% isobutane, 0.07% butane, 0.03% higher hydrocarbons), was provided by TGS, Bahía Blanca, Argentina. Chromatographic grade (99.999% molar) hydrogen and nitrogen; analytical grade (99.99% molar) air and argon, and helium (5.0 ultra-pure grade) were provided by AGA, Argentina. Commercial sunflower oil (98% (w/w) triglycerides plus 2% of mono-, di- and non-glyceride compounds) was maintained

* Corresponding author. Tel.: +54 0291 4861700; fax: +54 0291 4871600.
E-mail address: piqueras.martin@gmail.com (C.M. Piqueras).

0896-8446/$ – see front matter © 2009 Elsevier B.V. All rights reserved.
doi:10.1016/j.supflu.2009.05.005

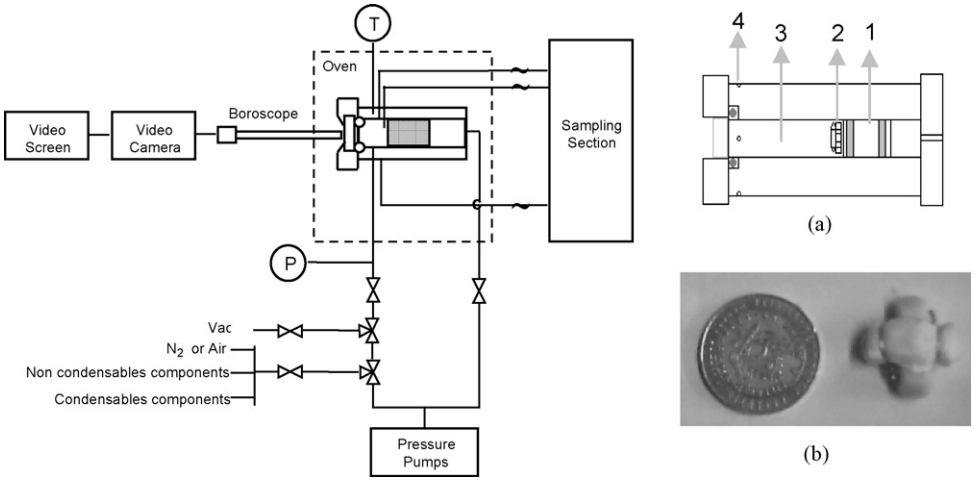

Fig. 1. Simplified flow-diagram of the batch cell. P, pressure transducer and readout; T, platinum resistance thermometer and readout. The sampling lines are heated traced. (a) Detail of the high pressure cell, 1: moveable piston; 2: magnetic stirrer with catalyst fixed on it; 3: reaction zone, 4: sampling connections. (b) Picture of the magnetic stirrer with the reduced catalyst enclosed in paper. The picture compares the stirrer device respect to a peso coin (around 18 mm).

in a nitrogen atmosphere and used without previous treatment. The triglyceride (TG) mixture had the following initial fatty acid composition: 7.94% C16:0 (palmitic), 4.22% C18:0 (stearic), 23.06% C18:1 (oleic), 64.44% C18:2 (linoleic), 0.17% C18:3 (linolenic), 0.54% C20:0 (eicosanoic), 0.64% C22:0 (docosanoic), with a corresponding iodine value (IV) of 131.4. The catalyst used for this reaction was Pd/γ-Al_2O_3 (Condea Puralox; 148 $m^2\,g^{-1}$; 200 μm particle diameter; average pore size 9 nm and pore volume 0.005 $cm^3\,g^{-1}$), with a metal loading and metal particle size of 0.77% (w/w) and 1.9 nm respectively. The metal precursor was palladium acetylacetonate $Pd(C_5H_7O_2)_2$, provided by Alpha.

2.2. Experimental set-up and procedure

The experiments were carried out in a variable-volume batch cell [7] schematically described in Fig. 1. The cell volume (excluding the piston volume) was 23.4 cm^3 and consists of three parts: a window-cap, a cell body, and an end-cap. A sapphire window (12 mm, thick) was fixed to the cell body by the window-cap. The original cell [7] was designed to work with mixtures of polymers and light alkanes, and had to be modified in order to avoid leakages when working with mixtures of lower viscosity. For this purpose, TEFLON O-rings were placed at both ends of the cell, and an additional one was added at the front of the cell body to get a better seal at the sapphire window. A new movable piston, made of stainless steel and covered with aluminum to prevent it from scratching the highly polished surface of the bore, was assembled to the cell. The piston has two TEFLON O-rings that could be pressed against the bore surface to prevent the pressurizing fluid from leaking into the cell body. The whole system was tested for leakages, using a hydrogen/propane (50/50) mixture at 373 K and pressures up to 250 bar.

In each reaction the cell was loaded with a certain amount of sunflower oil, measured as the weight difference between the empty and loaded cell, using a six-digit scale (Ohaus model Adventure). Then, the cell was evacuated (10^{-3} Torr), filled with 0.1 MPa propane, and evacuated again. A known amount of liquid propane was then loaded into the cell from the high-pressure manual generator, by measuring the displacement of the shaft, while maintaining the pump at constant temperature. The cell was heated up to the reaction temperature at a rate of 5 K min^{-1} and after that it was stabilized. At this point, a gas pulse was introduced through the hydrogen line, with the necessary pressure to reach the desired molar composition, considering this action as zero time run. This loading procedure gave an average error of 3% in the hydrogen composition. This was found out by performing separate reaction experiments, in which an excess of catalyst was used in order to consume all the hydrogen fed to the cell.

The sampling line was located near to the sapphire window (see Fig. 1(a)), and samples were withdraw under a well-stirred medium (agitation speed from 850 to 1000 rpm), which ensures were absolutely random. The procedure was carried out using one of the four ports of the cell, placed in the middle of the bore diameter. The sampling line was a capillary stainless steel tube of 1/16′ external and 1/64′ internal diameter and 78 cm of length. The line volume ascends to 95 μl by which a loop of 55 μl (45 cm of the same tube) is used. Each sample was 28 ± 6 mg depending on the cell pressure. The line was purged twice prior to actual sampling using the Valco six-way zero volume valve. This was found to be sufficient to clear the line. All the sampling line was heated at the cell temperature, in order to avoid obstruction. During this procedure, any pressure drop inside the cell was compensated by moving the piston manually through the pressure pump, maintaining the working pressure within a narrow range of variation (±0.1 MPa). Seven samples were withdrawn in each experiment, which represented about 10% of the total cell volume.

Six to ten milligrams of Pd catalyst were reduced in flowing hydrogen (75 $cm^3\,min^{-1}$) at 403 K during 1 h. After that, the catalyst was covered with 50–100 mg of hydrogenated sunflower oil (iodine number IV = 50) to prevent any contact with oxygen. With this cover, the catalyst was located onto the stirring device using a filter paper of Millipore grade 101 (pore size 2.5 μm). This configuration mimics the spinning basket reactors (see Fig. 1(b), it is compared with a one peso coin).

The samples were analyzed by capillary gas chromatography (Hewlett Packard 4890) using a Supelco SP-2560 chromatographic column, which allows the distinction between *cis* and *trans* geometrical isomers. The fatty acid composition and iodine value (IV) were determined following the AOCS Ce 1c-89 official method and recommended practice AOCS Cd 1c-85 respectively, derivatizating the samples by the IUPAC 2301 method. Peaks were assigned according to Sulpelco 37 FAME mix standard (catalog number 47885-U). The amount of hydrogen consumed during the reactions was calculated by following the degree of saturation achieved in the TGs, as given by the fatty acid composition of each sample. Conversion (x_{DB}) was defined as the quantity of double bonds, compared to the initially present in the TG.

3. Phase equilibria and thermodynamic modeling

3.1. Phase behavior of the system $H_2 + C_3H_8 + TG$

The phase behavior of this system can be quite complex. Severe changes in density and solubility with temperature, pressure and composition can be expected, because of the presence of a near-critical or supercritical solvent in a mixture with a permanent gas and a heavy liquid component. The large differences in molecular size and volatility between these components are likely to give rise to liquid phase-split and multiphase behavior [8].

Hydrogen solubility is low in compounds like liquid propane and triglycerides, and increases with temperature and pressure [9,10]. On the other hand, hydrogen and propane are completely miscible at a temperature above the critical temperature of propane.

Triglycerides (TGs) contain three long hydrocarbon chains linked to a glycerol backbone which represents only a small fraction of the compound molecular weight (i.e. 15%). This leads to a paraffinic behavior of TGs. For this reason the phase behavior of the binary propane + TGs is quite similar to that of propane + high molecular weight alkanes [11]. These systems show Type V fluid-phase behavior in the classification of Van Konynenberg and Scott [12]. Liquid–liquid (*l*–*l*) immiscibility and a liquid–liquid–vapor (*l*–*l*–*v*) locus appear at temperatures close to propane critical one. For example, in propane + tripalmitin mixtures the liquid–liquid–vapor equilibrium line extends from 349 K (lower critical end point, LCEP) to 370 K (upper critical end point, UCEP) [13]. The mutual solubility of both compounds increases with pressure and decreases with temperature [13,14].

The addition of hydrogen to the C_3H_8 + TG binary raises the pressure of the liquid partial miscibility limits, due to the low solubility of the gas in both compounds. An increase of 6 MPa in the critical pressure was observed, after adding a 4.5% hydrogen molar fraction to this binary [14].

Fig. 2 shows a schematic phase diagram of the ternary system (H_2 + C_3H_8 + TG), derived from the corresponding *P*–*x* binary diagrams at a temperature at which it is possible to have partial liquid miscibility in the binary propane + TG [14]. At pressure P_1, the ternary system shows a Type II phase diagram [15], having partial miscibility in two binary axis (see Fig. 2(a)). Liquid partial miscibility in the C_3H_8 + TG pair and liquid–vapor equilibria in the H_2–TG binary, give rises to a three-phase *l*–*l*–*v* zone in the ternary diagram. At a pressure P_2 above the maximum of the C_3H_8 + TG partial miscibility region, the ternary system is of Type I and has only one partially miscible pair (H_2 + TG), as shown in Fig. 2(b). There is a homogeneous region at high propane concentrations [16,17], where hydrogen and TGs are completely miscible. Fig. 2(c) shows the minimum propane concentration required to assure homogeneity of the reaction mixture at any H_2/TG ratio (horizontal dashed line) [16,17]. The black zone in the diagram indicates the adequate working region for a single-phase hydrogenation process. This is delimited by the minimum H_2/TG molar ratio required for the hydrogenation and by the minimum solvent molar composition.

3.2. Thermodynamic modeling

Knowledge of the phase boundaries of the multicomponent reaction system containing the supercritical solvent, hydrogen, the substrate to be hydrogenated and the reaction products is desired in order to have a scenario of the temperature and pressure limits that guarantee a certain phase condition. In the particular case of the hydrogenation of fatty oils, reactants and products are of similar chemical nature; i.e. they are basically high molecular weight triglycerides, differing only in the degree of unsaturation. Therefore, it is expected that the phase boundaries of the real reactant system could be modeled by a representative H_2 + C_3H_8 + TG ternary system [16,17].

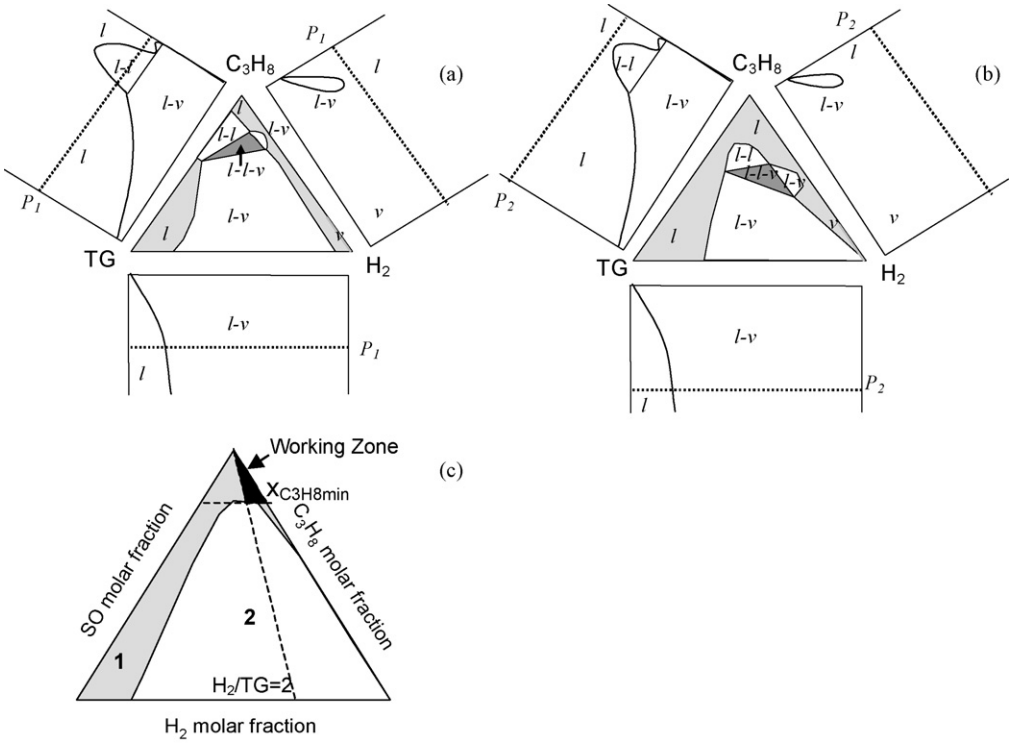

Fig. 2. Schematic ternary Gibbs phase diagrams derived from the corresponding *P*–*x* binaries at $T < 373.15$ K. Liquid (*l*), vapor (*v*), partial liquid miscibility (*l*–*l*), liquid–liquid–vapor equilibrium (*l*–*l*–*v*). (a) At P_1 (e.g. 10 MPa) liquid–liquid and vapor–liquid equilibrium in the binaries C_3H_8–TG and H_2–TG respectively, (b) At P_2 (e.g. 15.0 MPa) > P_1 liquid–liquid phase-split between C_3H_8 and TG disappears, (c) Adequate working region for the homogeneous hydrogenation (373.15 K, 160 bar), xC_3H_8min = 0.913, minimum C_3H_8 molar fraction to work in single-phase.

Table 1
GC-EoS functional groups and parameters.

Functional group	T^* (K)	q	g^*	g'
CH_3	600	0.848	316,910	−0.9274
CH_2	600	0.54	356,080	−0.8755
CH_3COO	600	1.728	831,400	−1.093
H_2	33.2	0.571	179,460	−0.0843
CH=CH	600	0.867	403,590	−0.7631
TG	600	3.948	346,350	−1.346
C_3H_8	369.8	2.236	436,890	−0.463

Interaction parameters

i	j	$k_{ij}{}^*$	$k_{ij}{}'$	α_{ij}	α_{ji}
CH_2/CH_3	CH_2/CH_3	1.0	0.0	0.0	0.0
H_2	CH_2/CH_3	1.0	0.0	11.846	11.846
CH_2/CH_3	CH=CH	1.0	0.0	0.0	0.0
CH_2/CH_3	TG	0.86	0.0	0.0	0.0
CH_2/CH_3	C_3H_8	1.0	0.0	0.0	0.0
H_2	CH=CH	1.0	0.0	0.0	0.0
H_2	TG	1.0	0.0	−10.144	−10.144
H_2	C_3H_8	1.243	0.0	−1.0	−1.0
CH=CH	TG	0.883	0.0	0.0	0.0
CH=CH	C_3H_8	1.0	0.0	0.0	0.0
TG	C_3H_8	0.86	0.0	0.0	0.0

	H_2	C_3H_8	TG x_{DB} = 0%	TG x_{DB} = 50%
dc (cm mol^{-1})	2.672	4.017	11.741	11.81

In the present work, the phase equilibrium boundaries were predicted by using a group-contribution equation of state GC-EoS [18,19]. Group-contribution methods are suitable for modeling fatty oil mixtures since the natural oil can be represented by a pseudo-triglyceride containing the same iodine value (IV) and saponification index (S) of the real multicomponent oil [10]. Table 1 shows the functional groups used to represent the molecules contained in the reaction mixtures. The table also gives the values of the parameters representative of each functional group: characteristic temperature (T^*), surface area (q) and energy (g^* and g'), binary interaction (k^* and k') and non-randomness parameters (α). The critical diameter (d_c) denotes the molecular size of each compound [18]. The parameter values shown in Table 1 were taken from the literature [16–20].

Routines supported by Michelsen's [21,22] minimization algorithm were used to calculate phase envelopes and multiphase separations of the ternary system ($H_2 + C_3H_8 + TG$) at different temperatures, pressures and compositions. With these tools, the working conditions and the evolution of each run during the whole reaction period could be predicted and followed.

Fig. 3 shows the measured [24] and calculated phase envelopes of the ternary ($H_2 + C_3H_8 + TG$), for four different isopleths having hydrogen molar fractions between 5.1 and 10.3%. Each curve shows a change in the slope, typical of transitions from vapor–liquid (l–v) to liquid–liquid (l–l) equilibrium conditions, with a vapor–liquid–liquid (l–l–v) equilibrium point at the intersection of the two sectors. For each composition, the one-phase region is located above the corresponding phase envelope. Fig. 3(a) shows the complete phase envelopes predicted by the GC-EoS equation, while Fig. 3(b) expands the region experimentally measured. The agreement between the experimental data and the predictions is high. Hence, the GC-EoS model can be employed to calculate the phase conditions in the range of temperature, pressure and compositions studied in this work.

Table 2
Working conditions applied to study the effect of temperature and pressure in the contents of *trans*-isomers and saturated TGs.

Molar fraction	H_2	C_3H_8	Oil
Average	6.78	90.85	2.48
Standard dev. (σ), N = 20	0.40	0.43	0.12
Working temperatures (K)		323, 338, 343, 374, 393	
Working pressures (MPa)		6.5, 11.3, 13.6, 16.3, 18.3	

4. Results and discussion

A series of experiments were carried out at different temperatures, pressures and H_2/TG feed ratios, in order to observe the effect of these variables on the activity and selectivity of the reaction. The temperature range was selected in order to achieve the activation of the metal catalyst. Conversion (x_{DB}) was not allowed to be higher than 50% hydrogenation of the double bonds. It is generally accepted that TG hydrogenation occurs in sequential steps, hydrogenating first all the linoleic fatty acids to oleic ones, without oleic consumption and stearic production. When almost all linoleic were consumed, a maximum amount of oleic happens and conversion is about 45–50%. It is known that a 1:3 *cis-trans* ratio occurs in the thermodynamics equilibrium between these isomers [23]. So, in oleic chains a large amount of isomerization occurs. In order to observe the C18:1 *trans* production, this should be done in the range of conversion from 0 to 50%, since a higher conversion values oleic fatty acids became the main reactant.

4.1. Variation of temperature and pressure

Five different temperatures from 353 to 393 K and pressures from 6.5 to 18.5 MPa were selected in order to observe the effect of these variables on the reaction behavior. A series of hydrogenation experiments were carried out with reaction mixtures having the average molar compositions reported in Table 2. This table also gives the standard deviations in the molar fractions of each component. A catalyst loading of 0.00131% (w/w) Pd/TG ratio was used.

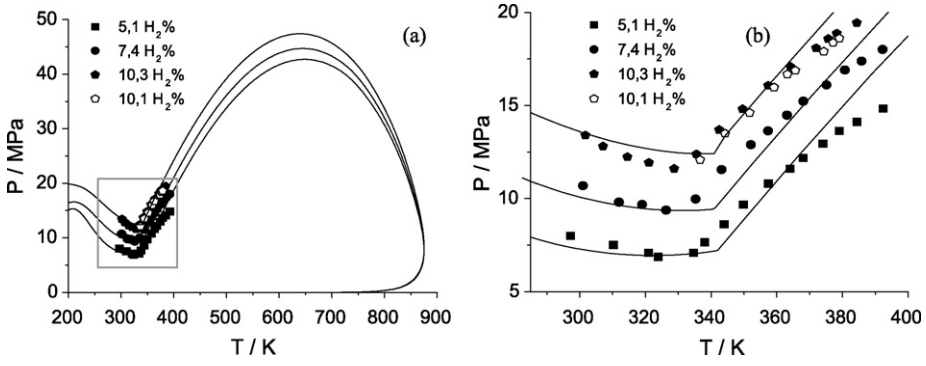

Fig. 3. $H_2 + C_3H_8 + TG$ phase envelopes of isopleths with H_2 molar fractions 5.1, 7.4, 10.1 and 10.3% molar. Experimental critical points (symbols) and GC-ENVEL predictions (lines). The second series at 10% H_2 was performed in order to compare the results at the most difficult condition to seal the cell.

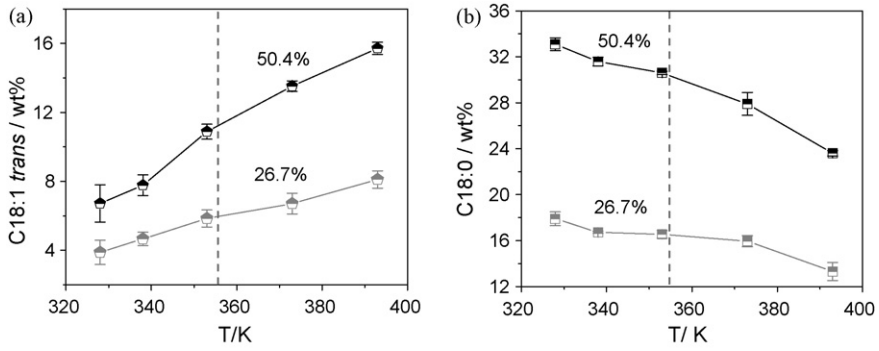

Fig. 4. C18:1 *trans* (Elaidic fatty acid) (a) and C18:0 (saturated fatty acid) (b) contents as a function of temperature, initial molar fraction of 6.78% H_2 + 90.75% C_3H_8 + 2.48% oil and 11 MPa. Vertical dashed lines indicate the phase-split limit at the beginning of the reaction: homogeneous (left), two-liquid phase condition (right).

Fig. 4(a) shows the variation of the C18:1 *trans* contents with temperature. The experiments were carried out at 11 MPa, for two different reaction conversions: 26.7 and 50.4%. When final conversions laid outside these values, the data were interpolated using fourth order polynomial equations with $R^2 > 0.99$ in all cases. The C18.1 *trans* amount increases with temperature, as it is generally reported in the literature [25].

For x_{BD} = 26.7%, the lowest *trans* content was 4.0% at the lowest temperature (328 K); but the reaction rate at this condition was low ($0.0059\ mol_{H_2}\ g_{cat}^{-1}\ min^{-1}$). For the same conversion, the highest level of C18:1 *trans* was 8.2% at 393 K. These values are higher than those reported by Ramirez [26], who performed the reaction under similar conditions also using propane as the solvent. At higher conversions (x_{BD} = 50.4%), the *trans* isomers content varied between 6.8% (at 328 K) and 15.7% (at 393 K), similar to the values found by Macher [27] in the hydrogenation of canola oil at 343 K, using a continuous reactor and propane as the solvent.

Fig. 4(b) shows the C:18.0 fatty acid content in the products. For the highest conversion studied, the ratio between the content of saturated TGs in the products and in the reactants lies between 3.5 and 4.5 at 328 and 393 K respectively. This represents a low selectivity to the poly-unsaturated fatty acids, indicating a high availability of hydrogen at the catalyst surface, as a consequence of both, higher H_2 concentration and better mass transport from the bulk of the fluid to the active sites of the catalyst.

Fig. 5 shows the effect of pressure in the contents of the products at 373 K and x_{DB} = 50.4%. The influence of pressure is rather low, since an increase of 14 MPa results in a difference of 2% in the isomerization products, while the stearic content oscillates around 31%, with a variation of almost 1%. Within these same limits, the change in density of the reaction mixture is of the order of 12% (396.5–446.4 g cm^{-3}), as predicted by the GC-EoS equation.

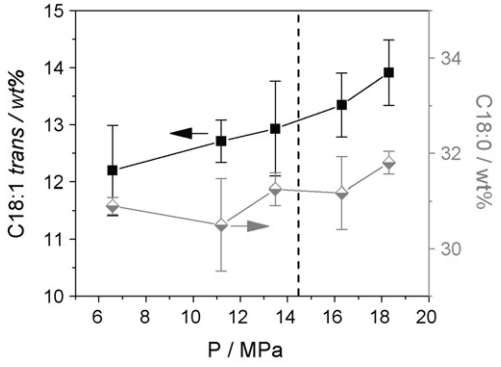

Fig. 5. C18:1 *trans* and C18:0 contents as a function of pressure, initial composition of 6.78% H_2 + 90.75% C_3H_8 + 2.48% oil, at 373 K and 50% conversion. Dashed line at 14.5 MPa indicate the phase-split limit: two-phase condition to the left; single-phase to the right.

4.2. Variation of the hydrogen/oil feed ratio

In order to observe the effect of the H_2/oil feed ratio on the reaction performance, several experiments were carried out changing this ratio from 1 to 10. Table 3 shows the experimental molar fractions fed to the reactor at each feed ratio, and the working temperature and pressure. The catalyst loading was Pd/TG = 0.00134%. The results are compared at similar conversion levels (10.6, 26.7 and 50.4%). When conversions fell outside these values, the experimental results were either interpolated or extrapolated to the selected values, using the procedure already mentioned in a preceding paragraph.

Fig. 6(a) shows the weight percentage of C18:1 *trans* for different H_2/oil molar feed ratios. An increase in the feed ratio produced a slight change in the isomerization. These results are consistent with

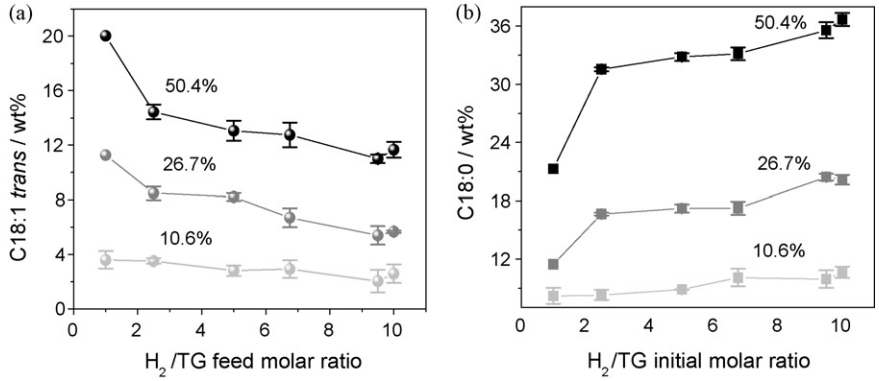

Fig. 6. C18:1 *trans* (a) and C18:0 (b) content as a function of the H_2/oil feed ratio.

Table 3
Temperature, pressure and compositions used to study the effect of H_2/oil feed ratio in the reaction performance.

H_2/oil feed ratio	H_2	C_3H_8	Oil
1.04	2.82	94.48	2.70
0.99	2.68	94.62	2.70
2.53	6.58	90.82	2.60
2.62	6.90	90.61	2.59
5.47	8.99	89.37	1.64
5.13	8.48	89.87	1.65
6.52	9.02	89.60	1.38
6.99	9.09	89.61	1.30
9.67	10.28	88.65	1.06
9.07	11.04	87.75	1.22
10.28	15.63	82.85	1.52
10.17	10.77	88.17	1.06
Working temperature (K)		373 ± 0.5	
Working pressure (MPa)		16.3 ± 0.1	

those already discussed. The high contents of isomers obtained for H_2/TG = 1 at the higher conversions, are in agreement with the fact that the amount of hydrogen is not enough to hydrogenate the double bonds beyond a 22% conversion level. As a consequence, the isomerization reaction is favored [25]. The C18.1 *trans* content was 11%, for a 50.4% conversion, at a H_2/oil ratio = 10. This value is slightly lower than the one reported by Macher [27] for a similar amount of H_2 in the feed (i.e. 16% for IV = 65 and H_2/canola oil = 10–15). Similar arguments are valid for the production of saturated TGs, as can be seen in Fig. 6(b).

4.3. Phase equilibrium analysis

As the hydrogenation reaction proceeds, hydrogen is consumed and the pressure required to reach total solubility in the ternary mixture decreases remarkably. In order to verify the phase equilibrium conditions during the reaction, it is necessary to know the phase boundaries of the reaction mixture at the beginning and at the end of the hydrogenation. The location of the experimental temperature and pressure in these phase diagrams indicates the phase conditions of the reaction mixture during the experiment.

Fig. 7 shows two-phase envelopes calculated with the GC-EoS model for a feed composition of 6.78% H_2 + 90.75% C_3H_8 + 2.48% oil and for the reaction mixture at 50% conversion (1.2% H_2 + 96.33% C_3H_8 + 2.48%). The calculations were made for a sunflower oil having an initial iodine number IV = 66.

The dots in Fig. 7 indicate the experimental temperature and pressure. The temperature was controlled within ±0.5 K of the set-point, while the pressure was maintained ±0.1 MPa around the selected value varying the volume. The dots can be separated in three different groups: the first one includes points 1–5; the second one, points 6 and 7 and the last one, points 8 and 9. In the first group, the reactions were performed under homogeneous conditions, because the system pressures lie always above the phase boundaries. The reactions of the third group were carried out under two-phase conditions, because the experimental pressures are below the 50% conversion phase boundary. The second group

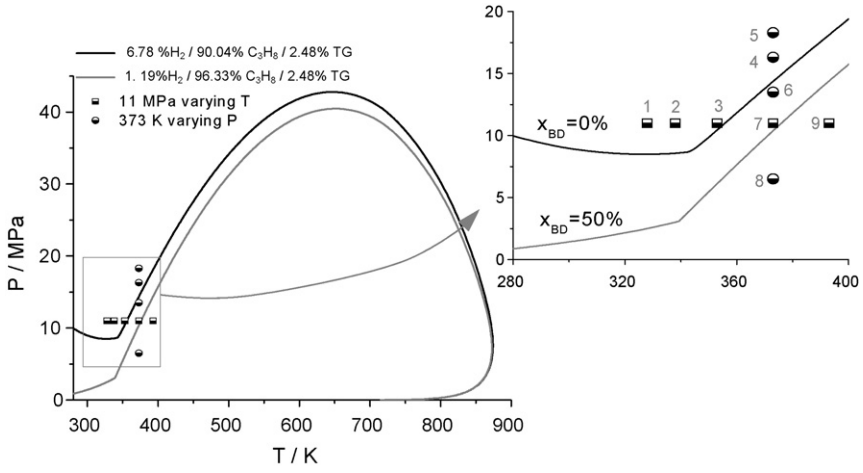

Fig. 7. Phase envelopes of the feed and 50% conversion isopleths, calculated with the GC-EoS model. The half-open symbols indicate the experimental conditions at which reactions were carried out.

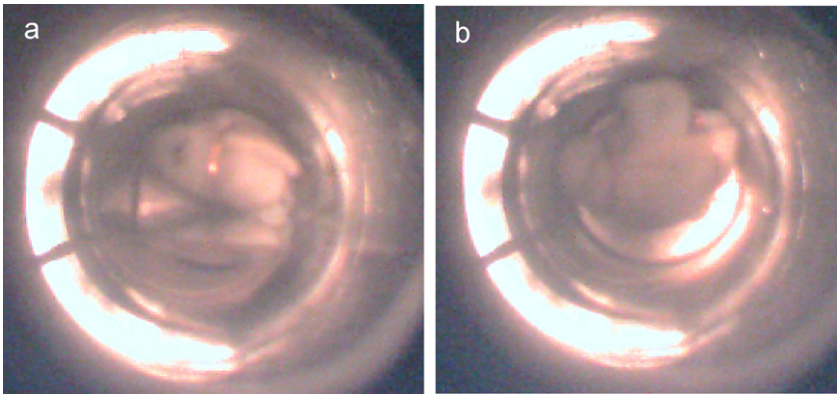

Fig. 8. Pictures of the reaction mixture at 11.2 MPa and 373 K. (a) Initial condition, (b) intermediate period (between 36 and 43% conversion). Both pictures were taken without stirring.

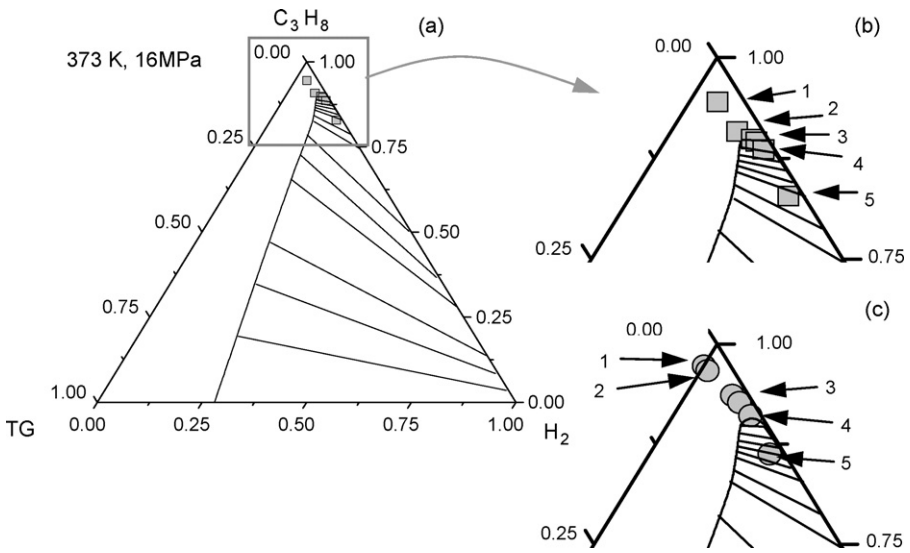

Fig. 9. Gibbs phase diagram of the reaction mixture at 16.3 MPa and 373 K. (b) The filled rectangles represent the initial molar fractions of each component (H_2/C_3H_8/TG) in the reaction mixture: (1) 2.82/94.48/2.70; (2) 6.58/90.82/2.60; (3) 8.48/89.87/1.65 and 9.02/89.60/1.38; (4) 10.28/88.65/1.06; (5) 15.63/82.85/1.52. (c) The filled circles correspond to the molar fractions at 50% conversion: (1) 0.0/97.30/2.70; (2) 0.69/96.71/2.60; (3) 4.74/93.61/1.65 and 5.89/92.72/1.38; (4) 7.88/91.05/1.06; (5) 12.19/86.29/1.52.

corresponds to reactions that initiated under a two-phase region and finished at homogenous conditions. This was visually verified (see Fig. 8) for the reaction carried out at 11.2 MPa and 373 K (corresponding to point 7 in Fig. 7). Two liquid-like phases separated by a meniscus can be seen in Fig. 8(a), while Fig. 8(b) shows a single-phase condition near the end of the reaction.

Fig. 9 represents the Gibbs phase diagram of the ternary system at 373 K and 16.3 MPa, calculated with the GC-EoS equation. The one-phase region is located above the binodal curve, which presents a maximum at 0.907 propane molar fraction. The symbols in this figure correspond to the initial (squares) and final (circles) compositions in the series of experiments carried out at different H_2/oil molar ratios and up to 50% conversion. Reactions with initial H_2/oil molar ratios equal to 1.04 and 2.53 (numbers 1 and 2 respectively, in Fig. 9) remained under a single-phase all the time. The opposite was true for the reaction with a feed ratio of 10.28 (point 5 in the figure). At the intermediate ratio values (points 3 and 4) the phase condition changed from a two-phase (initial) to a one-phase (final) state. This was experimentally verified as it is shown in Fig. 10 for the reaction with an initial composition of 8.48% H_2 + 89.87% C_3H_8 + 1.65% oil (corresponding to point 3 in Fig. 9). Fig. 10(a) shows two phases separated by a meniscus at the beginning of the reaction, changing to a homogeneous phase (Fig. 10(b)) after half-time of the reaction.

4.4. Mass-transport discussion

A significant observation from the results above is that, despite the phase transitions occurring during the reactions, either: selectivity to *trans* isomers or to saturated fatty acids changes smoothly. The vertical dashed lines in Fig. 4(a) and (b) indicate the phase-split limits at 11 MPa, for a mixture with initial molar fractions of 6.78% H_2 + 90.75 C_3H_8 + 2.48 oil. A two-phase condition is obtained to the right (i.e. above 356 K) while a homogeneous phase occurs to the left, below 356 K. *Trans* isomers and stearic fatty acid contents changed gradually. The same happens when pressure variation is analyzed (see Fig. 5). Total miscibility is reached at 373 K, for pressures higher than 14.5 MPa.

Similar results are observed by looking at the changes in the reaction rate with temperature and pressure. Fig. 11 shows the reaction rates at 25.7% conversion (calculated according to the IV measured for the samples withdrawn, which is directly related to the consumption of hydrogen and averaged over the reaction time needed to reach the specific value of conversion). Above 14.4 MPa (left axis) and below 356 K (right axis) the reaction mixture is under single-phase conditions. There is a smooth variation of the reaction rate with both, temperature and pressure. The same type of results regarding reaction rates and product distribution were found by other authors working with well-stirred reactors [26,27].

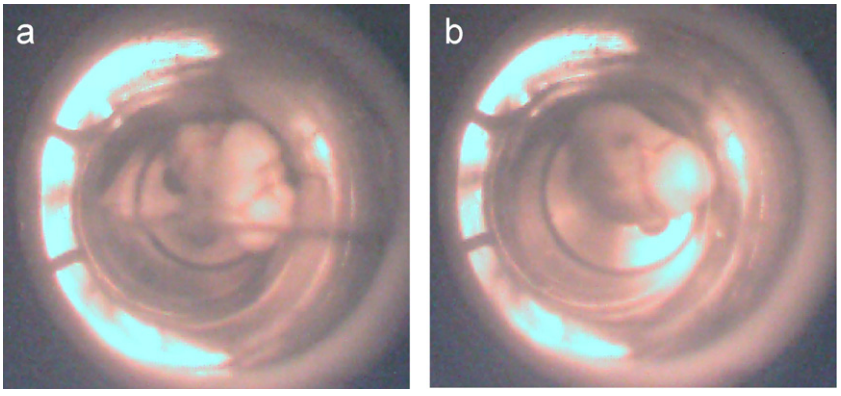

Fig. 10. Pictures of a reaction mixture having an initial composition of 8.48% H_2 + 89.87% C_3H_8 + 1.65% oil at 373 K and 16.2 MPa. (a) Two-phase as initial condition. (b) Single-phase as condition at conversion about 48%.

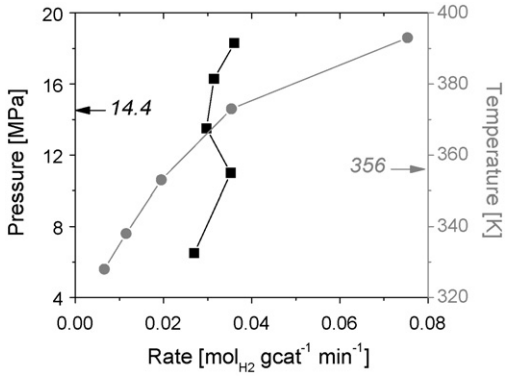

Fig. 11. Reaction rates for temperature and pressure variation measured at 25% double bond conversion. The rate was based on the moles of double bond converted averaged on the time needed to reach this conversion and the palladium weight.

den Hark and Harrod [29] studied the hydrogenation of fatty acid methyl esters (FAME) to produce fatty alcohols. The reactions were carried out in a continuous reactor, under supercritical propane. These authors observed a linear increase in the apparent rate of FAME consumption, for substrate feed concentrations of up to 1% molar. Under these conditions the reaction rate was of the same order of magnitude of gas-phase hydrogenations [30]. On the other hand, when the substrate concentration reached 1.5–2%, a sudden decrease of the rate as well as the FAME conversion was observed. This was accompanied by an abrupt increase of the pressure drop inside the fixed-bed reactor. These drastic changes in the system behavior were attributed to the transition of the reaction medium from homogenous to heterogeneous conditions. The authors speculated that the catalyst pores were blocked by the condensed substrate-rich phase, making it difficult for the hydrogen-rich phase to access to the active sites. The situation becomes similar to conventional hydrogenation, because hydrogen should be transferred throughout a gas–liquid interface, reducing its concentration at the catalyst surface. The phase-split has a crucial effect in the system mass transport: there is a sudden increase in viscosity, from 0.053 mPa s (similar to pure C_3H_8) to almost 1.5 mPa s (typical of FAME) [29].

The apparent discrepancy between the results found in the present paper and those reported by den Hark and Harrod [29] regarding the effect of phase-split on the reaction rate, can be found in the mass transport associated to the flow regime in each type of reactor (batch and fixed-bed respectively). In a fixed-bed reactor the global reaction rate is limited by the external mass transfer [31].

The external mass transfer coefficients in a film around a spherical catalyst particle were calculated for both types of reactors, at the corresponding experimental flow regimes. The calculations for the batch reactor were made for the hydrogenation of sunflower oil at 373 K and 6.5 MPa, with an initial global composition of 6.78% H_2 + 90.75% C_3H_8 + 2.48% oil. The mass transfer coefficient in the fixed-bed reactor was calculated for the hydrogenation of FAME at 353 K and 15.2 MPa [29]. Methylpalmitate (MP) was chosen to represent the real FAME mixture [32], and the global molar fractions of the reactants were 20% H_2 + 78% propane + 2% methylpalmitate.

Table 4 reports the results of the calculations. The compositions and densities of the phases (P_1 and P_2) at equilibrium were calculated with the GC-EoS equation. The table shows the dimensionless numbers characterizing both, the hydrogen- and substrate-rich phases. The viscosities of the pure components and their mixtures were estimated by the Lucas and Letsou-Stiel correlations [33]. The Sherwood number was calculated with Frossling correlation [31]. The Reynolds number determines the difference in mass flow between both reactors. The fixed-bed reactor operates under poor forced mixing, which becomes evident by the Sherwood number

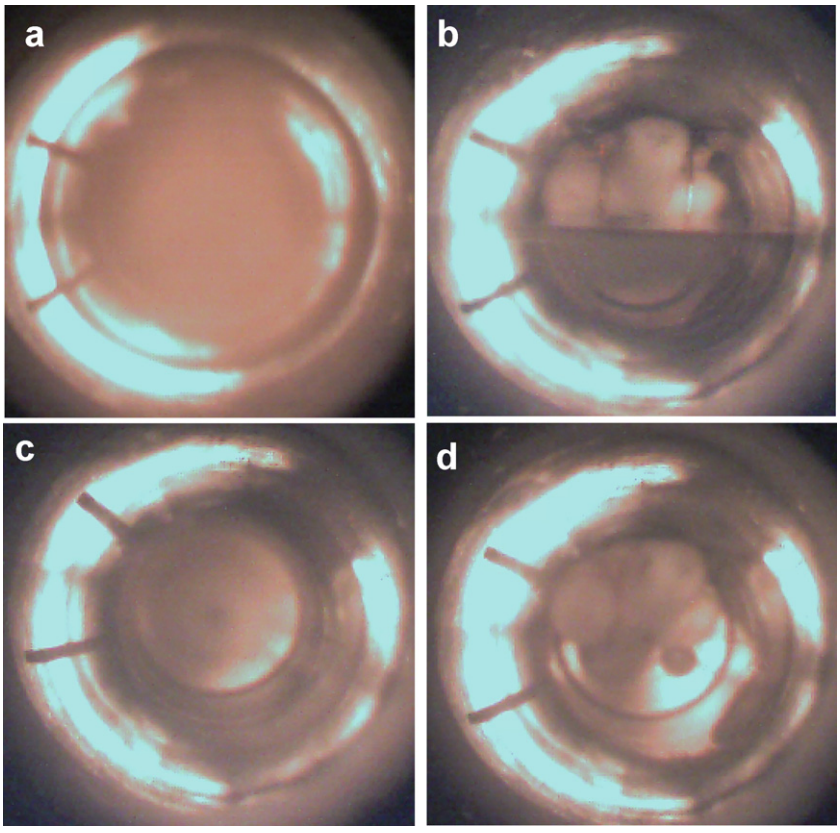

Fig. 12. Pictures of the reactant mixture and homogeneous conditions: (a) Two-phase system at 850 rpm stirring speed. (b) Same system without stirring H_2-rich phase (P_1) above, substrate-rich phase (P_2) below. (c) Homogeneous system at 800 rpm. (d) Same system without stirring.

Table 4
Mass transfer properties in the hydrogenation of triglycerides (TG) and fatty acid methyl esters (FAME) carried out in a batch and a continuous reactor respectively.

Parameter	P_1 TG	P_2 TG	P_1 FAME	P_2 FAME	FAME
H_2% molar	8.70	1.94	39.24	16.48	
C_3H_8% molar	91.30	89.39	60.71	81.16	
Substrate (TG or MP) % molar	1.7×10^{-7}	8.68	0.05	2.36	
Dp (μm)	200	200	400	400	400
ρ (kg/m^3)	184.9	500.9	157.4	319.3	841[a]
μ (mPa s)	0.05	0.35	0.03	0.07	0.15[b]
$\eta \times 10^7$ (m^2 s^{-1})	2.75	7.01	2.07	2.27	1.78
U (m s^{-1})	0.942[c]	0.942[c]	0.001[b]	0.001[b]	0.001[b]
Re	1371.2	538.0	1.8	1.6	0.4
Sc_{H2}	0.27	0.70	0.21	0.23	–
$Sc_{TG\ and\ MP}$	13.75	35.03	10.34	11.35	89.29
Sh_{H_2}	16.45	14.36	2.48	2.47	–
$k_s \times 10^2$ (m s^{-1})	8.21	7.19	0.61	0.60	–
$Sh_{TG\ and\ MP}$	55.18	47.49	3.76	3.73	2.26
$k_{s\ TG\ and\ MP} \times 10^3$ (m s^{-1})	5.52	4.75	0.19	0.19	0.11

Using $Deff_{TG\ or\ MP} = 2 \times 10^{-8}$ m^2 s^{-1} from criterion of Refs. [28,29,35].
[a] From Ref. [35].
[b] From Ref. [29].
[c] Empiric correlations for stirred tanks from Ref. [31]. The diffusion coefficients were obtained from Refs. [28,29]. H_2 and C_3H_8 pure properties from Ref. [36].

close to 2 [34]. For this reactor the calculated mass transfer coefficients in both phases are more than one order of magnitude lower than those in the batch reactor. For comparison, Table 4 also reports the estimated coefficient for pure FAME, which agrees with the value reported by den Hark and Harrod (2×10^{-4} m/s [29,35]). The values of the Reynolds and Schmidt numbers in the batch reactor are indicative of a good mixing regime, which would induce a close contact between both fluid phases.

The pictures in Fig. 12 show the flow regime inside the batch reactor working under a biphasic condition. Fig. 12(a) shows the reaction mixture stirred at 850 rpm. The cloudy image illustrates a good contact between very small drops in both phases. Even though it is not possible to detect a flow pattern, it should be reasonable to imagine a twister-like movement around the cells axis. Fig. 12(b) shows the H_2-rich and the TG-rich phases, separated by a meniscus, when stirring is stopped. The magnetic stirrer is visible like a white piece at the top of the image. For comparison, Fig. 12(c) and (d) shows the corresponding flow patterns when the reaction mixture is under homogeneous conditions.

The difference in the mixing regimes between the continuous and batch reactors results in different external mass transfer limitations. The excellent mass transfer reached in the discontinuous reactor because of the forced mixing, makes the global reaction rate and selectivity insensitive to the environment phase condition. Taking account the results, we could then conclude that internal mass transfer inside the catalyst pores should be equally efficient in both, the homogeneous and two-phase conditions.

From Table 4 it becomes evident that the TG concentration in the H_2-rich phase P_1 is negligible. Furthermore the concentration of H_2 in the TG-rich phase P_2 would be able to convert only 5% of the total double bonds in this phase if no H_2 transference between both phases were possible. Since H_2 diffusivity is almost 100 times greater than TG diffusivity [29,35], we suppose that the main part of the reaction occurs in the TG-rich phase, with most of the hydrogen coming from phase P_1. A minor contribution to the reaction could take place in the hydrogen-rich phase as a result of the TG movement. A more detailed study of the mass transfer between phases is needed since we consider this work as preliminary study.

5. Conclusions

The reaction rate and product distribution were analyzed at different temperatures, pressures and H_2/oil feed ratios, which involves different phase equilibrium scenario. Compared to the gas–liquid hydrogenation process, lower selectivity to polyunsaturated fatty acids was obtained, which implies low *trans* isomers production and high saturated fatty acids contents. These results agree with a high H_2 concentration at the internal surface of the catalyst, as a consequence of improved mass transfer. The transition from homogeneous to biphasic conditions has no effect on the reaction activity and selectivity, which implies very high mass transfer coefficients of the reactants at the external surface as well as in the internal pore structure of the catalyst. In this hand, solvent addition raises the mass transfer of the medium. A comparison was made between the mass transfer coefficients in batch and fixed-bed reactors. The results confirmed that reactions carried out in a continuous flow reactor without a highly forced mixing require single-phase conditions, constrained by the high pressures needed to reach this solubility state. On the other hand, well stirred reactors (i.e. continuous tank or batch reactor) are efficient when working at lower pressures under biphasic conditions.

References

[1] A. Baiker, Supercritical fluids in heterogeneous catalysis, Chem. Rev. 99 (1999) 453–473.
[2] M. Perrut, Supercritical fluid applications: industrial developments and economic issues, Ind. Eng. Chem. Res. 39 (2000) 4531–4535.
[3] A. Bolz, U.K. Deiters, C.J. Peters, T.W. de Loos, Nomenclature for phase diagrams with particular reference to vapour-liquid and liquid–liquid equilibria, Pure Appl. Chem. 70 (1998) 2233–2257.
[4] R. Wandeler, N. Künzle, M.S. Schneider, T. Mallat, A. Baiker, Continuous enantioselective hydrogenation of ethyl pyruvate in "supercritical" ethane: relation between phase behavior and catalytic performance, J. Catal. 200 (2000) 377–388.
[5] S. Pereda, S. Bottini, E. Brignole, Supercritical fluids and phase behavior in heterogeneous gas–liquid catalytic reactions, Appl. Catal. A: Gen. 281 (2005) 129–137.
[6] D. Kromhout, A. Menotti, B. Bloemberg, C. Aravanis, H. Blackburn, R. Buzina, A.S. Dontas, F. Fidanza, S. Giaipaoli, A. Jansen, M. Karvonen, M. Katan, A. Nissinen, S. Nedeljkovic, J. Pekkanen, M. Pekkarinen, S. Punsar, L. Rasanen, B. Simic, H. Toshima, Dietary saturated and trans fatty acids and cholesterol and 25-year mortality from coronary heart disease: the Seven Countries Study, Prev. Med. 24 (1995) 308–315.
[7] S.J. Chen, R.E. Randelman, R.L. Seldomridge, M. Radosz, Mass spectrometer composition probe for batch cell studies of supercritical fluid phase equilibria, J. Chem. Eng. Data 38 (1993) 211–216.
[8] C.J. Peters, Multiphase equilibria in near-critical solvents, in: E. Kiran, J.M.H. Levelt Sengers (Eds.), Supercritical Fluids: Fundamental for Application, Kluwer Academic Publishers, Dordrecht, 1994, p. 117.
[9] W.L. Burriss, N.T. Hsu, H.H. Reamer, B.H. Sage, Phase behavior of the hydrogen-propane system, Ind. Eng. Chem. 45 (1953) 210–213.
[10] J. Wisniak, L.F. Albright, Kinetics of the hydrogenation of rapeseed oil: II. Rate equations of chemical reactions, Ind. Eng. Chem. 53 (1961) 375–380.
[11] S.B. Bottini, T. Fornari, E.A. Brignole, Phase equilibrium modelling of triglycerides with near critical solvents, Fluid Phase Equilibr. 158–160 (1999) 211–218.
[12] P.H. Van Konynenberg, R.L. Scott, Critical lines and phase equilibria in binary van der waals mixtures, Philos. Trans. R. Soc. Lond., Ser. A 298 (1980) 495.
[13] H.G.A. Coorens, C.J. Peters, J. de Swaan Arons, Phase equilibria in binary mixtures of propane and tripalmitin, Fluid Phase Equilibr. 40 (1988) 135–151.
[14] L.J. Rovetto, S.B. Bottini, E.A. Brignole, C.J. Peters, Supercritical hydrogenation processes Experimental results on the fluid phase behavior of binary and ternary mixtures of hydrogen, propane and tripalmitin, J. Supercrit. Fluids 25 (2003) 165–176.
[15] J.M. Sorensen, T. Magnussen, P. Rasmussen, A. Fredenslund, Liquid–liquid equilibrium data—their retrieval, correlation and prediction, Fluid Phase Equilibr. 2 (1979) 297–309.
[16] S. Pereda, Ingeniería del Equilibrio entre Fases: Aplicación a Reactores de Hidrogenación Supercrítica, Ph.D. Thesis Universidad Nacional del Sur, Bahía Blanca, Argentina, 2003.
[17] S. Pereda, S.B. Bottini, E.A. Brignole, Phase equilibrium engineering of supercritical hydrogenation reactors, AIChE J. 48 (2002) 2635–2645.
[18] S. Skjold-Jørgensen, Gas solubility calculations II. Application of a new group-contribution equation of state, Fluid Phase Equilibr. 16 (1984) 317–351.
[19] S. Skjold-Jørgensen, Group contribution equation of state (GC-EOS): a predictive method for phase equilibrium computations over wide ranges of temperature and pressures up to 30 MPa, Ind. Eng. Chem. Res. 27 (1988) 110–118.
[20] S. Espinosa, T. Fornari, S.B. Bottini, E.A. Brignole, Phase equilibria in mixtures of fatty oils and derivatives with near critical fluids using the GC-EOS model, J. Supercrit. Fluids 23 (2002) 91–102.
[21] M. Michelsen, The isothermal flash problem Part I. Stability, Fluid Phase Equilibr. 9 (1982) 1–19.

[22] M. Michelsen, The isothermal flash problem Part II. Phase-split calculation, Fluid Phase Equilibr. 9 (1982 b) 21–40.
[23] R.J. Grau, A.E. Cassano, M.A. Baltanas, Kinetics of methyl oleate catalytic hydrogenation with quantitative evaluation of cis-trans isomerization equilibrium, Ind. Eng. Chem. Res. 26 (1) (1987) 18–22.
[24] C.M. Piqueras, Control de isómeros *trans* en la hidrogenación de aceites comestibles: aplicación de propano supercrítico como medio de reacción, Ph.D. Thesis, Universidad Nacional del Sur, Bahía Blanca, Argentina, 2008.
[25] R.R. Allen, Hydrogenation, in: D. Swern (Ed.), Bailey's Industrial Oil and Fat Products, fourth ed., Wiley, New York, 1982.
[26] E. Ramirez Rangel, Contribution to the Study of Heterogeneous Catalytic Reactions in SCFs: Hydrogenation of Sunflower Oil in Pd Catalysts at Single-Phase Conditions. Ph.D. Thesis Universitat Politècnica de Catalunya, Barcelona, Spain, 2005.
[27] J.W. King, R.L. Holliday, G.R. List, J.M. Snyder, Hydrogenation of vegetable oils using mixtures of supercritical carbon dioxide and hydrogen, J. Am. Oil. Chem. Soc. 78 (2001) 107–113.
[28] M. Macher, Supercritical Hydrogenation of Vegetable Oils, Ph.D. Thesis, Chalmers University of Technology, Göteborg, Sweden, 2001.
[29] S.V. den Hark, M. Harrod, Fixed-bed hydrogenation at supercritical conditions to form fatty alcohols: the dramatic effects caused by phase transitions in the reactor, Ind. Eng. Chem. Res. 40 (2001) 5052–5057.
[30] M.-B. Macher, J. Höögberg, P. Møller, M. Härröd, Partial hydrogenation of fatty acid methyl esters at supercritical conditions, Fett/Lipid 101 (1999) 301–305.
[31] H.S. Fogler, Elements of Chemical Reaction Engineering, third ed., Prentice Hall, New Jersey, 1999.
[32] S. Pereda, S.B. Bottini, E.A. Brignole, Gas–liquid reactions under supercritical conditions—phase equilibria and thermodynamic modeling, Fluid Phase Equilibr. 194–197 (2002) 493–499.
[33] R.C. Reid, J.M. Prausnitz, B.E. Poling, Properties of Gases and Liquids, fourth ed., McGraw-Hill, New York, 1986.
[34] K. Westerterp, W. van Swaaij, A. Beenackers, Chemical Reactor Design and Operation, second ed., Jhon Wiley Sons, New York, 1984, pp. 448–451.
[35] S. Van der Hark, The Use of Supercritical Fluids to Reduce the Number of Phases in Catalytic Hydrogenation: The Reaction of Fatty Acid Methyl Esther to Fatty Alcohols, Ph.D. Thesis, Chalmers University of Technology, Göteborg, 2000, p.70.
[36] T.E. Daubert, R.P. Danner, Physical and Thermodinamic Properties of Pure Chemical Data Compilation, DIPPR-Taylor & Francis, Bristo, PA, 1994.